

Influence of Conformational Asymmetry on the Phase Behavior of Ternary Homopolymer/Block Copolymer Blends around the Bicontinuous Microemulsion Channel

Ning Zhou,[†] Timothy P. Lodge,^{*,†,‡} and Frank S. Bates^{*,†}

Department of Chemical Engineering & Materials Science and Department of Chemistry,
University of Minnesota, Minneapolis, Minnesota 55455

Received: October 6, 2005; In Final Form: January 6, 2006

We have developed a new ternary polymeric system, poly(ethylene-*alt*-propylene) (PEP)/poly(butylene oxide) (PBO)/PEP–PBO, to study the complex phase behavior near the bicontinuous microemulsion phase channel. The molecular weights of the PEP and PBO homopolymers are 2600 and 3050 g/mol, respectively, and the copolymer is 23.4 kg/mol with volume fraction composition $f_{\text{PBO}} = 0.49$. A combination of small-angle neutron scattering, small-angle X-ray scattering, rheology, optical microscopy, and visual oil bath measurements was employed to map out the phase diagrams at five fixed homopolymer PBO/PEP ratios, ranging from 40/60 to 60/40 by volume, with copolymer concentrations ranging from 0 to 100%. It was found that the bicontinuous microemulsion channel is consistently cut off at low temperature by a hexagonal phase. We attribute this phenomenon to the effect of the conformational asymmetry between the PEP and PBO species, whereby the more flexible PBO component induces a spontaneous curvature toward the PBO domains. These findings complement previous descriptions of the isopleth phase diagrams for A/B/A–B systems and identify a new design variable for preparing bicontinuous phases.

Introduction

Microemulsions tailored by amphiphilic interactions in surfactant systems are of considerable theoretical and industrial interest. Ternary mixtures of oil, water, and surfactant exhibit a rich variety of ordered and disordered morphologies. One particularly intriguing structured state is that of a bicontinuous microemulsion (B μ E) featuring two continuously interpenetrating phases, oil and water, with surfactants lying at the interface.¹ Its polymeric counterpart, consisting of two immiscible homopolymers and their corresponding diblock copolymer, has received significant attention since it was first uncovered about one decade ago.^{2–16} The most striking analogy in the phase diagrams of water/oil/surfactant systems and polymeric A/B/A–B blends is that the phase spaces of both types of B μ E are located between the lamellar and macrophase-separated regions.

Some efforts have been paid to seek the universal phase diagram of homopolymer A/homopolymer B/diblock copolymer A–B systems along the isopleth, where the two homopolymers are mixed in equal volumes.⁴ The existence of a B μ E phase channel has been proved experimentally to be a universal feature in the isopleth upon the investigation of a variety of systems with quite different molecular weights and distinct chemical structures.⁴ However, there are still two unresolved key issues regarding the B μ E phase channel: (i) How deep in temperature does the B μ E channel extend, and (ii) how does the B μ E terminate at low temperature? In this report, through a particular choice of monomers and molecular weights, we address these two issues.

The phase behavior of ternary homopolymer/block copolymer blends is influenced by an array of experimental variables that include component molecular weights and concentrations, block

copolymer composition, temperature, and pressure. Symmetric ternary mixtures can facilitate the understanding of their essential thermodynamic behavior. The symmetry condition of polymeric A/B/A–B systems includes: (i) two homopolymers of equal sizes ($N_A = N_B$) and equal concentrations ($\phi_A = \phi_B$), (ii) a compositionally symmetric diblock copolymer ($f_A = f_B = 0.5$), and (iii) conformational symmetry between the A and B species. For a particular system, the first two conditions are readily achievable through experimental manipulation but the third is an intrinsic characteristic of the system. Previous work^{2–8,13–14} has established the universal existence of the B μ E phase in the partially (satisfying conditions i and ii) symmetric systems. It is thus unclear whether conformational asymmetry can have an impact on the B μ E phase channel or not.

The importance of conformational asymmetry between different components has been realized in the fundamental thermodynamic study of many polymeric systems.^{17–24} For example, the conformational mismatch in binary polymer blends can drive the conformationally smaller or more flexible species to enrich the surface,^{17,18} and by a similar mechanism, the more flexible block of a diblock copolymer can preferentially segregate to the interface of the thin films.¹⁹ As another example, the mesophase boundaries of the phase diagram of diblock copolymers are shifted toward higher content of the more flexible block.^{21–23} The origin of these effects is purely entropic.

In this paper, we investigate a new ternary polymeric system, poly(ethylenepropylene) (PEP)/poly(butylene oxide) (PBO)/PEP–PBO, to experimentally reexamine the established universal phase diagram along the isopleth with particular emphasis on the phase behavior of the ternary mixtures around the B μ E phase channel. We reveal some new features in the isopleth, which complement and extend previous descriptions.^{2–8,13–14}

Experimental Section

Materials. A partially deuterated poly(ethylene propylene) (PEP) homopolymer was synthesized by anionic polymerization

* To whom correspondence should be addressed. E-mail: bates@cems.umn.edu; lodge@chem.umn.edu.

[†] Department of Chemical Engineering & Materials Science.

[‡] Department of Chemistry.

of isoprene in cyclohexane at 40 °C with *sec*-butyllithium as the initiator, followed by catalytic (Pd/CaCO₃) saturation with D₂ under ~500 psi in cyclohexane at 70 °C. The ¹H NMR (500 Hz) spectroscopy of the PEP shows no residual double bonds. Assuming each repeat unit of polyisoprene incorporates two deuterium atoms in the hydrogenation, the molar mass ($M_n = 2600$ g/mol) of the PEP was calculated on the basis of the molecular weight of the polyisoprene precursor, which was measured by size exclusion chromatography (SEC) with a light scattering detector. The synthesis procedure of the poly(butylene oxide) (PBO) homopolymer and PEP–PBO block copolymer will be described in more detail subsequently.²⁵ Briefly, the methoxyethanol and monohydroxyl-terminated polyisoprene (PI–OH) were converted to the corresponding potassium alkoxides and used as initiators for the anionic polymerization of the butylene oxide monomer in THF at 50–70 °C to prepare the PBO homopolymer and PI–PBO block copolymer, respectively. The PI–PBO block copolymer was then catalytically saturated with D₂ to yield the PEP–PBO block copolymer. The molar mass ($M_n = 3050$ g/mol) of the PBO homopolymer was measured by matrix-assisted laser desorption/ionization (MALDI) spectrometry. The total molecular weight of the PEP–PBO block copolymer is 23.4 kg/mol by SEC, and ¹H NMR was used to determine the volumetric composition $f_{\text{PBO}} = 0.49$, assuming the densities of the blocks are equal to those of the homopolymers. The polydispersity indexes M_w/M_n of all the polymers used here are less than 1.1, measured by SEC. The densities of PEP, PBO, and PEP–PBO were measured on a density gradient column at room temperature: 0.868, 0.954, and 0.917 g/mL, respectively. Both PEP and PBO are amorphous polymers with very low glass transition temperatures of approximately –60 °C.

The molar volumes of the two homopolymers are nearly equal ($M_{\text{PEP}}/\rho_{\text{PEP}} \approx M_{\text{PBO}}/\rho_{\text{PBO}} = V_H$), and the ratio of the molar volume of the homopolymers to the diblock copolymer is 0.12. The molecular weight of the diblock copolymer was designed to match its order–disorder transition (ODT) temperature (163 °C) to the critical temperature of the binary homopolymer blends ($T_c = 173$ °C).

Blend Preparation. Most of the ternary polymer blends were dissolved in benzene and stirred to form homogeneous solutions, followed by freeze-drying under vacuum to remove most of the solvent. To eliminate the residual solvent, the blends were then heated to 160 °C for 2 h and 80 °C for 2 days in a vacuum oven. Binary homopolymer blends and ternary blends with less than 12% block copolymer were dissolved in methylene chloride and then transferred to a 1.0 mL ampule. Most of the solvent was stripped off under a slow nitrogen stream, followed by heating to high temperatures under vacuum for complete drying. The ampule was then flame-sealed under vacuum after complete degassing for cloud point determination. The compositions of the polymer blends reported in this paper are in terms of volume fractions, based on the measured densities of the components at room temperature. The homopolymer PBO/PEP ratios of the ternary blends range from 40:60 to 60:40.

Rheology. Measurements were carried out with a strain-controlled Rheometric Scientific ARES rheometer. The samples were loaded between two parallel plates of 25 mm diameter under nitrogen. Before data collection, the samples were heated to the disordered state to eliminate any influence from sample loading, and then cooled to room temperature. Dynamical temperature ramps were performed at a heating rate of 1 or 2 °C/min, a frequency of 1 or 10 rad/s, and a constant strain amplitude of 5%.

Small-Angle X-ray Scattering. Cu K α and synchrotron SAXS experiments were carried out at the University of Minnesota and at the Advanced Photon Source, Argonne National Laboratory, respectively. Cu K α X-rays ($\lambda = 1.54$ Å) are generated by a Rigaku RU-200BVH rotating anode. Synchrotron radiation ($\lambda = 1.55$ Å) was selected from an undulator beam using a double-crystal monochromator, and highly collimated using two sets of slits located at 32 and 13 m upstream of the sample, each set to a square gap of 200 μm width. Samples were placed between two Kapton films spaced by a rubber O-ring of ~1.5 mm thickness. The sample holders were under helium atmosphere to avoid parasitic scattering and sample degradation. Sample loading sometimes aligns the blends and leads to an anisotropic scattering pattern. To produce isotropic patterns, samples were disordered in the SAXS beam line and then cooled to form ordered structures before SAXS measurements.

Small-Angle Neutron Scattering. SANS measurements were carried out at the National Institute for Standards and Technology (NIST) in Gaithersburg, MD, on the NIST/Exxon/University of Minnesota 30 m instrument using $\lambda = 7$ Å wavelength neutrons ($\Delta\lambda/\lambda = 0.11$). The neutron scattering contrast between the PEP (D₂-saturated polyisoprene) and PBO is sufficient to produce acceptable scattering patterns after 5 min exposure times. The completely dried polymer blends were prepared as described above and directly loaded into quartz cells with stainless steel spacers of 1.02 mm thickness, which were sealed using high-temperature silicone glue. All samples produced nearly azimuthally isotropic two-dimensional (2D) scattering patterns that were averaged to 1D plots of intensity vs the magnitude of scattering wave vector ($q = 4\pi \sin(\theta/2)/\lambda$ where θ is the scattering angle). The scattering data were corrected for background and cell scattering, detector sensitivity, sample thickness, and transmission. The absolute differential scattering cross section per unit sample volume (cm⁻¹) was calculated using previously reported calibration techniques.²⁶

Cloud Point Measurement. For polymer mixtures prepared in ampules, the cloud points were determined using a custom-built oil bath. The temperature of the oil bath was increased to 180 °C, and the ampules were shaken vigorously to homogenize the blends. Then, the temperature was lowered in 5 °C increments and equilibrated for several minutes at each temperature. The blends became opaque quickly below the cloud points. After the phase-separation temperatures were estimated, the blends were reheated to one phase and slowly cooled in 1 °C increments with longer equilibration times. Binary homopolymer blends within 5% of the critical composition phase separated into two layers of approximately equal volume very quickly when the temperature was just a few degrees below the cloud point. For ternary blends with more than 12% block copolymer, an optical microscope (Olympus BX51) was employed to determine phase-separation temperatures. At room temperature, these samples were cloudy but did not phase separate into bulk layers because of kinetic barriers. The samples were placed into 50 μm thick spacers between one glass disk and one slide cover. A Linkam DSC was used as the sample holder to control the temperature, and a nitrogen atmosphere was provided to prevent sample degradation. Cloud points on the homopolymer rich side of the B μ E phase channel were determined by decreasing temperature, whereas the cloud points on the copolymer rich side and the bottom of the B μ E phase channel were measured by increasing temperature.

Results

The PEP/PBO system was chosen for the present study because it has the following advantages: (i) both components are amorphous with very low T_g (approximately $-60\text{ }^\circ\text{C}$), which provides a large, accessible temperature window, (ii) PEP and PBO have reasonable scattering contrast for both SAXS and SANS, and (iii) the moderate Flory–Huggins χ parameter of this system results in relatively low molecular weights of the two homopolymers and the diblock copolymer to access the disordered or one-phase region. The blends therefore have relatively low viscosities and high diffusivities and reach equilibrium states within short times.

For the phase diagrams at fixed PBO/PEP ratios, the ODT and order–order transition temperatures were determined using the SAXS beam line at the University of Minnesota. One-phase/macrophase-separated boundaries were studied using visual oil bath and optical microscopy. The narrow two-phase region of lamellae-hexagonal coexistence is not regarded as macrophase separated. Details of the macrophase-separated region, such as the boundaries between the two-phase and three-phase regions, are not investigated in this study.

Diblock Copolymer. The SAXS pattern of the pure diblock copolymer PEP–PBO at room temperature is shown in Figure 1a. Two scattering peaks were observed at relative q values of 1 and 3, which are associated with a lamellar microstructure. The scattering extinction or suppression of the second-order peak in the SAXS profile is due to the overlap of the Bragg peak and the minimum in the form factor of a symmetric lamellar structure with equal volumes of the alternating layers. This is consistent with the composition of the diblock copolymer. The lamellar spacing d is $232\text{ }\text{\AA}$ at $25\text{ }^\circ\text{C}$ and $202\text{ }\text{\AA}$ at $160\text{ }^\circ\text{C}$, calculated with $d = 2\pi/q^*$, where q^* is the magnitude of the scattering vector of the first-order peak. The block copolymer chain is less stretched to form the lamellar structure at higher temperatures, resulting in a smaller domain size. The ODT was observed between 160 and $165\text{ }^\circ\text{C}$ using SAXS (Figure 1b), where there is an abrupt change in the peak intensity and peak width. The dynamic temperature ramp (Figure 1c) was also performed to investigate the ODT, concomitant with a sharp drop in the dynamic elastic and loss moduli. The interaction parameter χ at the ODT temperature can be estimated by $(\chi N)_{\text{ODT}} = 10.5$ (mean-field theory): 0.032 .

Binary Homopolymer Blends. The phase-separation temperatures of the binary homopolymer blends presented in Figure 2 were determined by using visual oil bath measurements. The blends exhibit typical upper solution critical temperature (USCT) behavior since there is no specific interaction, such as hydrogen bonding. The cloud points were used to construct the coexistence curve, which were analyzed with the mean-field Flory–Huggins theory²⁷ and nonmean-field Guggenheim fit²⁸ (eq 1).

$$|\phi - \phi_c| \propto \left(1 - \frac{T}{T_c}\right)^\beta \quad (1)$$

The dashed curve in Figure 2 is the binodal well fitted by the Flory–Huggins theory ($\beta = 1/2$) with a critical PBO volume fraction ϕ_c of 0.52 , a critical temperature T_c of $174\text{ }^\circ\text{C}$, and a χ parameter of $(75.6/T - 0.117)$, where T is the temperature in Kelvin. The fitted ϕ_c is very close to the theoretical one of 0.49 , calculated by

$$\phi_c = \frac{\sqrt{\nu_{\text{PEP}}}}{\sqrt{\nu_{\text{PEP}}} + \sqrt{\nu_{\text{PBO}}}} \quad (2)$$

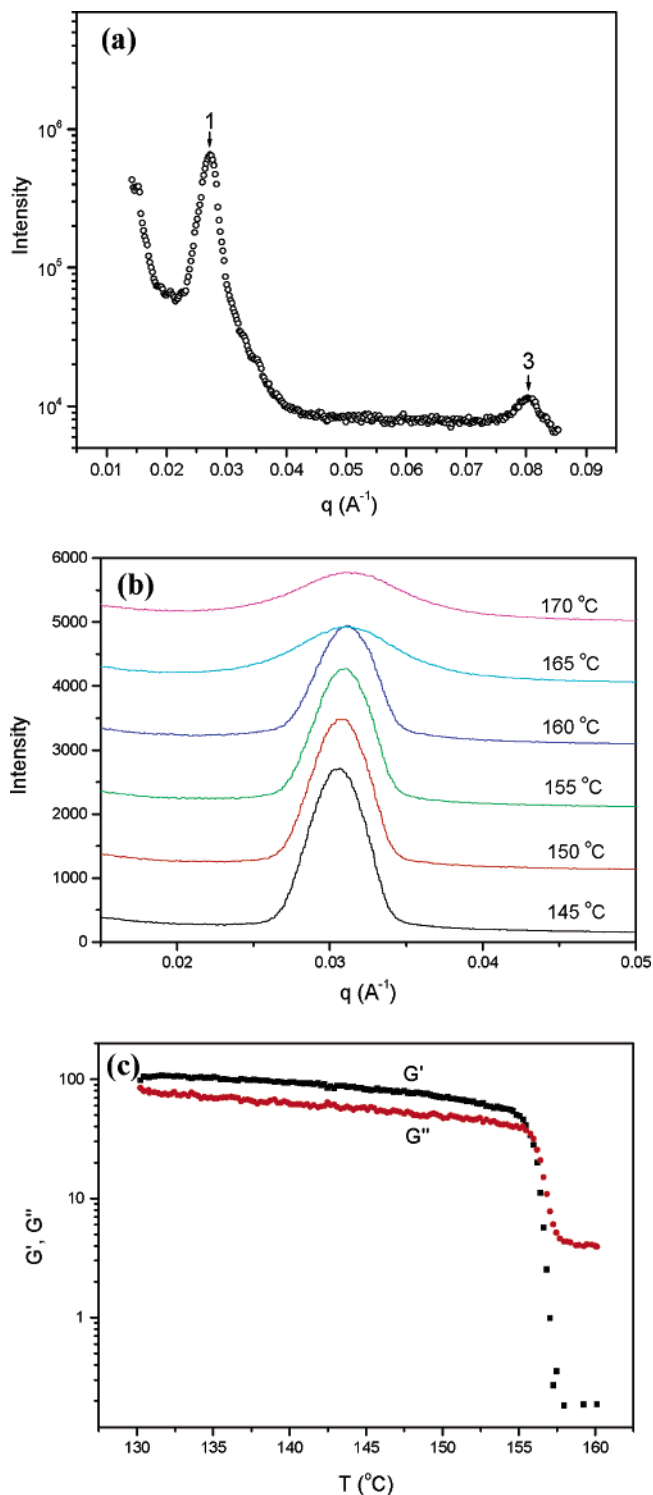


Figure 1. (a) SAXS pattern of the neat PEP–PBO block copolymer at room temperature. (b) SAXS patterns taken in $5\text{ }^\circ\text{C}$ intervals for the PEP–PBO. Profiles are shifted for clarity. (c) Dynamic temperature ramp data of the PEP–PBO.

where ν_{PEP} and ν_{PBO} are the molar volumes of the two homopolymers. The solid curve in Figure 2 corresponds to a Guggenheim fit based on eq 1. In accordance with this fitting, $\phi_c = 0.51$, $T_c = 173\text{ }^\circ\text{C}$, and $\beta = 0.30$. The mean-field and Guggenheim fits result in nearly the same ϕ_c and T_c , but the latter appears to match the experimental data better. For the low-molecular-weight ($\sim 3\text{ kg/mol}$) blends, the thermal and composition fluctuation should play a significant role in the phase-separation/one-phase transition and therefore leads to a

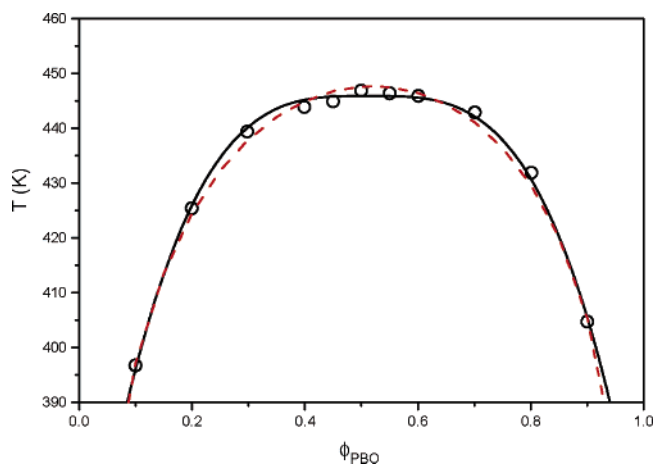


Figure 2. Cloud points of the binary homopolymer blends. The dashed and solid curves correspond to a binodal fit by mean-field Flory–Huggins theory and the Guggenheim fit, respectively.

deviation from the mean-field theory. The fitted critical exponent β of 0.30 is close to the universal value $\sim 1/3$ established in the gas–liquid and liquid–liquid coexistence curves of small molecules.²⁸

Phase Diagrams at Fixed Homopolymer Ratios. Five phase diagrams of the PEP/PBO/PEP–PBO system at fixed PBO/PEP ratios ranging from 40:60 to 60:40 are shown in parts a–e of Figure 3. At temperatures above 115 °C, the isopleth phase diagram with equal volumes of the two homopolymers (Figure 3c) is strikingly similar to the diagrams shown in previous work.⁴ Below 16% block copolymer, the ternary polymer blends were macrophase separated at temperatures below the cloud points. Above 17% block copolymer, the system adopted a symmetric lamellar microstructure below the ODT. Between 16% and 17% PEP–PBO, the blends formed one-phased polymeric $B\mu E$, the channel of which separates the lamellar and multiphase regimes. However, at temperatures below 115 °C, the isopleth phase diagram of the PEP/PBO/PEP–PBO system exhibits some new features, which are not evident in the established phase diagrams, such as the cutoff of the $B\mu E$ phase channel by hexagonally packed cylindrical phase, the phase transition and coexistence between symmetric lamellae and Hex cylinder, and the phase boundary of one-phased Hex and multiphases involving isotropic homopolymer-rich phases. Further discussion of the formation of the HEX phase in the isopleth will be made in the Discussion section. The overall features described above are also present in the phase diagrams at homopolymer ratios different than 1. In the following parts, we will refer to the phase diagrams at different homopolymer ratios as 40/60, 45/65, 50/50 (isopleth), 55/45, and 60/40 phase diagrams, corresponding to their respective PBO/PEP ratios.

On the homopolymer-rich side of the phase diagrams, visual oil bath and optical microscopy were used to determine the boundaries between the one-phase and phase-separated regions. For the ternary blends containing less than 12% diblock copolymer, we relied on visual oil bath cloud point measurements. The refractive index contrast between PEP and PBO components is large enough to observe the phase separation. All samples were heated to the one-phase region at 180 °C and held for 10–20 min resulting in specimen clarity. Upon slowly cooling, the samples became cloudy and ultimately split into two clear phases. Optical microscopy is a more sensitive technique and was employed for samples with more than 12% diblock copolymer. To the right (lower fractions of block copolymer) of the $B\mu E$ phase channel, phase separation only

involves isotropic liquidlike phases, such as homopolymer-rich phases and the $B\mu E$, which are of relatively low viscosity and high diffusivity. Therefore, these discrete phases rapidly segregated into domains of tens of micrometers over a period of several minutes, which can be easily observed. The cloud points of these samples were measured by cooling from the one-phase region in 5 °C intervals. Under and to the left of the $B\mu E$ channel, the phase separation was associated with one or two anisotropic solidlike phase(s), such as hexagonal cylinders and lamellae, which are relatively viscous. Consequently, it took 1 day or even longer for the phase separation to be observed under the microscope. Because of this kinetic issue, we determined the cloud points or dissolution points of these samples by heating from the phase-separated region in 10 °C intervals.²⁹ Upon heating above the phase-separation temperature, the interfaces between different phases disappeared gradually and the samples became optically clear within several hours. Although the optical microscope is powerful in cloud point measurement, it is unable to identify whether the polymer blends phase separated into two phases or three phases.

As described above, the line of phase-separation transitions in the phase diagrams can be divided into two categories. One is associated with only liquidlike phases, but the other is associated with one or two solidlike phase(s). The latter were not observed in the previous work on homopolymer A/homopolymer B/diblock copolymer A–B phase diagrams. The intersections of these two kinds of lines of transition in the 40/60, 45/55, 50/50, 55/45, and 60/40 phase diagrams correspond to block copolymer volume fractions of approximately 15.5%, 16.5%, 15.5%, 13.5%, and 13.5%, respectively. Therefore, with the addition of the block copolymer to the binary homopolymer blends, the 45/55 blend required the most diblock copolymer to saturate the PBO/PEP interface to form a $B\mu E$. We will discuss this further in the Discussion section.

On the block copolymer-rich side of the phase diagrams, the ODTs and order–order transitions were investigated using SAXS, SANS, and rheology. A representative example of the ODT determination for a 50/50 sample at $\Phi_H = 78\%$ using SAXS is shown in Figure 4. Upon heating from 122 to 138 °C in 2 °C intervals, the ODT of this blend coincides with a sharp drop of the peak intensity and a discontinuous increase of the peak width. These features of the ODT for the ternary blends are similar to those for the neat diblock copolymer PEP–PBO described previously. The ODT boundaries in the five phase diagrams were determined using the same method. Adding homopolymers into the pure diblock copolymer destabilizes the lamellar phase, resulting in a monotonic decrease of the ODT temperatures from 163 °C for the pure diblock copolymer to 125 °C for the 50/50 ternary blends containing $\Phi_H = 82\%$. Further addition of the homopolymers leads to the formation of a $B\mu E$, spanning about 2% wide in block copolymer composition along the isopleth phase diagram (parts c and f of Figure 3). The lower boundaries of the $B\mu E$ phase channels, the order-to- $B\mu E$ transition temperatures, were obtained via SAXS as well. As shown in Figure 3, these boundaries moved upward with increasing Φ_H , and thus exhibited the opposite trend in comparison with the normal ODT boundaries on the left-hand side of the $B\mu E$ phase channels. The left boundaries of the $B\mu E$ phase channels move to the higher fractions of the block copolymer as the ratio of homopolymer PBO to PEP decreases from 60:40 to 40:60, resulting in the widening of the $B\mu E$ phase channel. In other words, by holding the block copolymer concentration fixed, for example, $\Phi_H = 84\%$, the

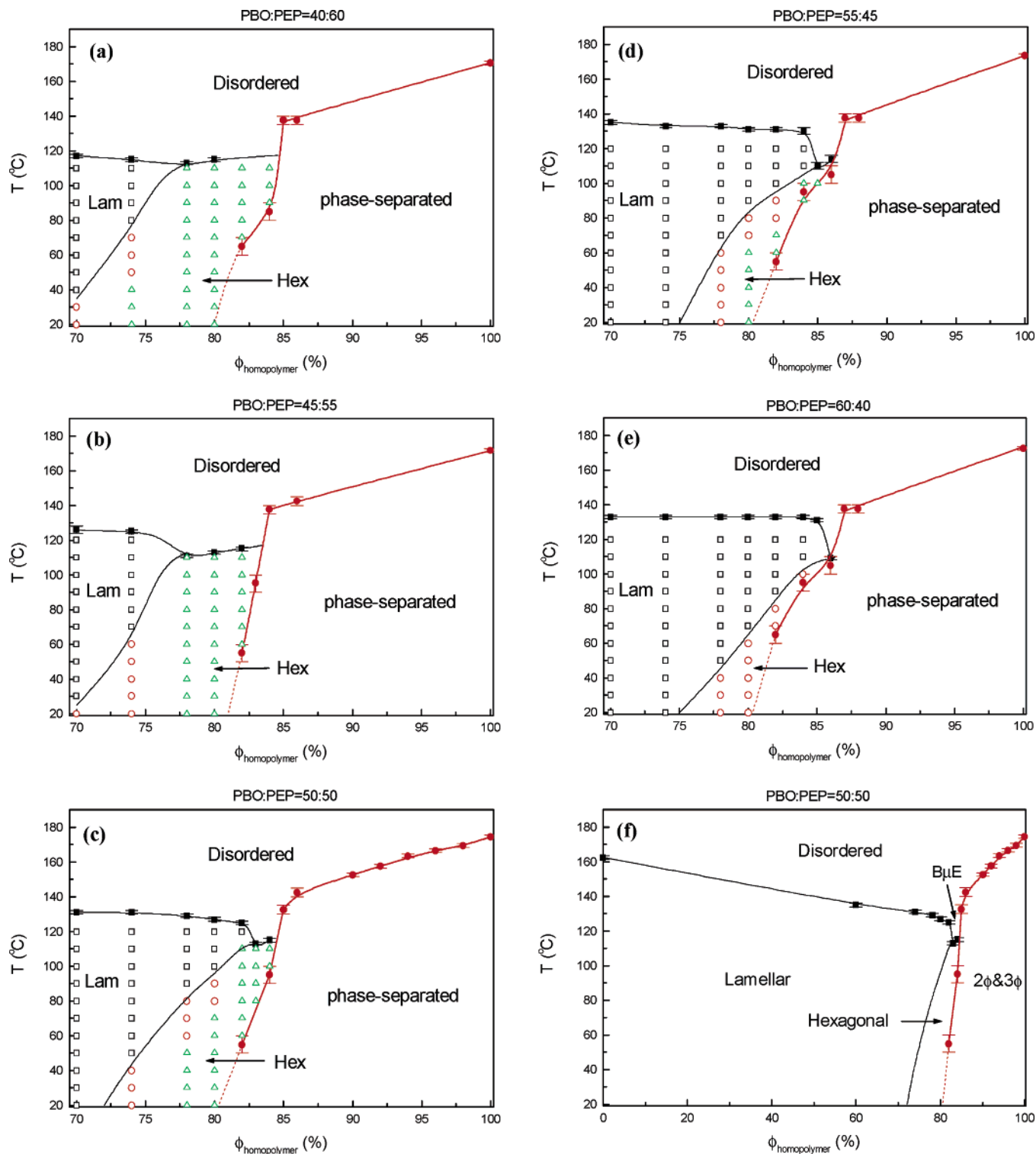


Figure 3. Phase diagrams for the ternary mixtures at fixed PBO/PEP ratios: (a) 40:60, (b) 45:55, (c) 50:50, (d) 55:45, and (e) 60:40. (f) Full phase diagram along the isopleth. The phase boundaries were determined by various methods: order–disorder transition investigated by SAXS (filled squares); macrophase separation investigated by a visual oil bath and optical microscope (filled circles); order–order transition investigated by SAXS with open squares, open circles, and open triangles representing the lamellar phase, the coexistence of the lamellar and hexagonal phases, and the hexagonally packed cylindrical phase, respectively.

amount of homopolymer PBO in the ternary mixtures decreases, leading to the stabilization of the $B_{\mu}E$ relative to the lamellar microstructures at high temperatures.

Small-angle neutron scattering experiments were carried out to characterize the $B_{\mu}E$ samples. The scattering profiles of 50/50 blends containing $\Phi_H = 83\%$ and $\Phi_H = 84\%$ at temperatures from 120 to 140 °C are shown in Figure 5. The scattering data

were fitted with the Teubner–Strey microemulsion model³⁰

$$I(q) = \frac{k}{a_2 + c_1 q^2 + c_2 q^4} \quad (3)$$

where $I(q)$ is the static scattering intensity as a function of q , the magnitude of the scattering wave vector, and k , a_2 , c_1 and

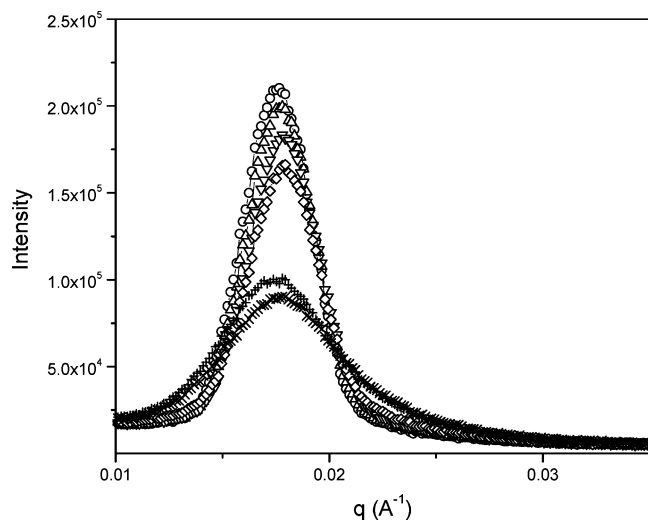


Figure 4. SAXS data determining the order–disorder transition temperature for a 50/50 sample containing 22% block copolymer ($\phi_{\text{PEP}} = \phi_{\text{PBO}} = 39\%$): 122 °C (○), 124 °C (△), 126 °C (▽), 128 °C (◇), 130 °C (+), and 132 °C (×). For clarity, SAXS data at other temperatures are not shown.

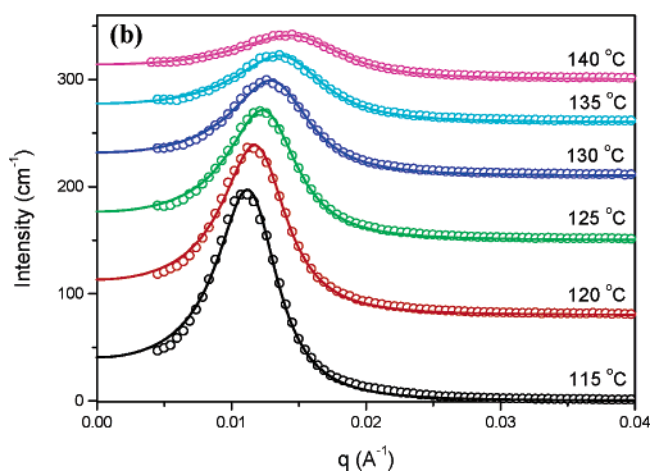
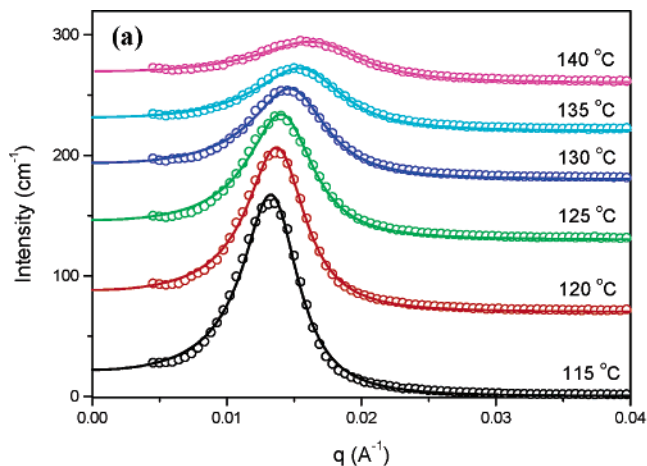


Figure 5. SANS patterns for 50/50 samples containing (a) 17% and (b) 16% block copolymer, at the indicated temperatures. The solid curves are the fits to the Teubner–Strey microemulsion model. The data are shifted for clarity.

c_2 are the associated coefficients. As evident in the Figure 5, all of the Teubner–Strey fits are rather good except for a systematic deviation at high q values, which is attributed to the scattering contribution from the Gaussian chains. The amphiphilicity factor, $f_a = c_1/(4a_2c_2)^{1/2}$, was calculated, which measures

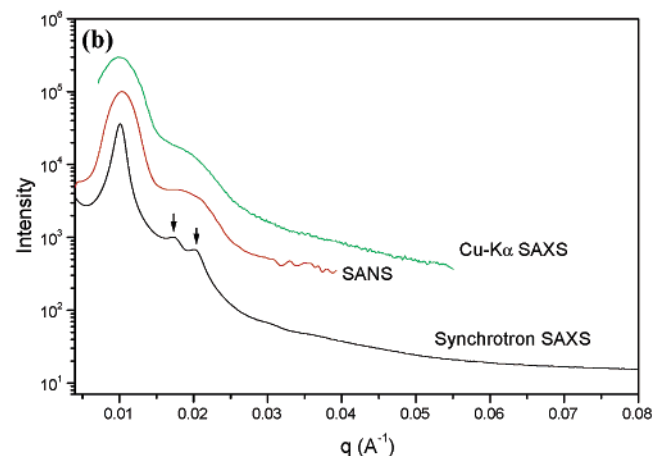
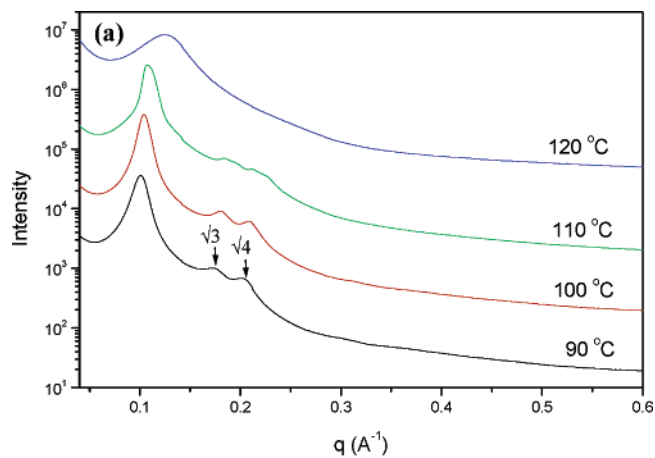


Figure 6. (a) Synchrotron SAXS patterns for the 50/50 sample containing 17% block copolymer, at indicated temperatures. The higher-order peaks at $\sqrt{3}q^*$ and $2q^*$ are denoted by arrows. Curves are shifted for clarity. (b) Comparison among the synchrotron SAXS pattern, Cu K α SAXS pattern, and SANS pattern of the same sample as in part a at 90 °C. Curves are shifted for clarity.

the structure strength of the microemulsion. (The ordered lamellar structure corresponds to $f_a = -1$, and the completely disordered state corresponds to $f_a = 1$.)³¹ As the 83% and 84% samples were heated from 115 to 140 °C, the amphiphilicity factors increased from -0.93 to -0.85 and from -0.89 to -0.81 , respectively. In this temperature range, both 83% and 84% microemulsions are highly structured, and the former with the higher block copolymer composition is more structured.

High-resolution synchrotron SAXS data of the 50/50 blend containing $\Phi_H = 83\%$ are shown in Figure 6a. Below the ODT (111 °C), three scattering peaks were observed with the q value ratio of $1:\sqrt{3}:\sqrt{4}$, consistent with a hexagonal phase. Similar scattering patterns (not shown) were obtained in the 50/50 sample at $\Phi_H = 84\%$. Therefore, the B μ E phase channel is cut off by a nonlamellar phase at low temperatures, which was not anticipated or considered in the previous analysis.^{2,4,5} Comparison of the SANS data, the Cu K α SAXS data taken at the University of Minnesota, and the synchrotron SAXS data of the same sample at 100 °C is made in Figure 6b. Only two scattering peaks with a q ratio of $1:2$ can be resolved in the SANS and Cu K α SAXS patterns, which might be used to mistakenly assign the sample to a lamellar structure. The broad, second, higher-order peak obtained in the relatively low-resolution techniques actually split into two clear peaks at $\sqrt{3}$ and $\sqrt{4}q^*$ in the high-resolution synchrotron SAXS. For a symmetric 50/50 sample, if it adopts a lamellar structure, then the even higher-order peaks ($2q^*$, $4q^*$, ...) will be suppressed

in the small-angle scattering profile. In accordance with this information, we can identify the morphologies of the symmetric or nearly symmetric ternary blends just using the Cu K α SAXS technique, which is very convenient. More specifically, the scattering peak q ratio of 1:3 corresponds to a lamellar phase, whereas the peak q ratio of 1:2 corresponds to a hexagonal phase. Using this analysis, we established the Lam–Hex transition boundaries in the ordering regions of the phase diagrams (Figure 3).

The Cu K α SAXS data of 50/50 blends at $\Phi_H = 70\%$, 74%, 78%, 80%, and 82% are shown in Figure 7. As the 70% sample was heated from 20 °C toward the ODT temperature (131 °C) (Figure 7a), the peak q ratio of 1:3 persisted, the principal peak intensities dropped continuously, and the q^* value increased progressively, indicating the 70% sample only adopted a lamellar structure. In contrast, the 78% sample behaved quite differently with increasing temperatures (Figure 7c). Below 50 °C, the peak q ratio was 1:2, consistent with the hexagonal phase. Above 90 °C, the peak ratio became 1:3, corresponding to a symmetric lamellar phase. Between 50 and 90 °C, coexistence between the Hex and Lam phases was identified with two principal q^* values. As shown in Figure 7c, the Hex-to-Lam phase transition of the 78% sample was associated with a loss of the “second” higher-order peak (or, more correctly, $\sqrt{3}$ and $\sqrt{4}$ q^* peaks) and a discontinuous change (sudden increase) of the q^* value. The order–order transitions of the 74%, 80%, and 82% samples exhibited similar features as shown in parts b, d, and e of Figure 7, respectively. In the isopleth phase diagram (Figure 3c), the Hex-to-Lam transitions occur at higher temperatures and the Hex–Lam coexistence temperature windows appear to narrow with the increase of the total homopolymers composition. For the 82% sample, the Hex–Lam coexistence was not observed (or was less than 5 °C wide) via Cu K α SAXS.

The thermally induced Hex-to-Lam transition was also investigated using rheology. A representative plot of G' and G'' for the 82% sample was shown in Figure 8. As the 82% blend was heated from 60 to 135 °C at a rate of 2 °C/min under 5% strain and 10 rad/s frequency, there were two phase transitions, a Hex-to-Lam transition at ~ 108 °C with a sudden drop of G' by about a factor of 3 and a Lam-to-Dis transition at ~ 122 °C with a sharp drop of G' by approximately 2 orders of magnitude, respectively, which are consistent with the SAXS results (Figure 7e). When the 82% sample adopts the hexagonal cylindrical structure at low temperatures, the system is solidlike with $G' > G''$, whereas when the 82% sample is lamella structured, it is more liquidlike with $G' < G''$. In the isopleth phase diagram, the symmetric lamellar phase is surprisingly replaced by a hexagonal phase at low temperatures. By the use of similar analysis, the details of the ordered phase regions of the other four different PBO/PEP ratios were established. As shown in Figure 3, the Lam/Hex boundaries progressively move to the right-hand side (higher Φ_H) as the homopolymer PBO/PEP ratios increase from 40:60 to 60:40, leading to the decrease in the extent of the hexagonal phase. Thus, at the same composition of the diblock copolymer and the same temperature, the Hex-to-Lam transition can be achieved by increasing the homopolymer PBO/PEP ratio, which suggests that the PBO component forms the core of the cylinder and the PEP component constitutes the continuous matrix phase.

Discussion

The isopleth phase diagram has been well studied among a wide variety of systems.^{2–8,13–14} Accordingly, a universal isopleth has been suggested with the existence of a $B\mu E$ phase

channel separating the lamellar phase and macrophase-separated region. However, the bottom boundaries of the $B\mu E$ phase channel were not accessed in most of the investigated systems due to the limited temperature window, which could be overcome by redesigning (increasing) the molecular weights of those blends to raise the one-phase/macrophase-separated boundary and/or the order–disorder transition boundary to high temperatures.

The formation of a polymeric $B\mu E$ near a mean-field Lifshitz point is attributed to the dramatic effect of fluctuations. As the temperature is lowered, the $B\mu E$ phase channel is predicted to eventually narrow because of the competition between the bending energy of the block copolymer-laden interfaces of the microemulsions and the diminishing effect of the thermal fluctuations. In the SANS study of the PEP/PEO/PEP–PEO system, Washburn et al.⁵ observed the coexistence of the $B\mu E$ and lamellar phases and that the $B\mu E$ channel narrows at low temperatures. On this basis, they deduced that the $B\mu E$ channel would disappear completely at lower temperatures and be substituted by the lamellar phase. This deduction might be incorrect, and the hexagonal phase could be more stable at lower temperatures relative to both $B\mu E$ and lamellar phases.

Hillmyer et al.⁴ observed a hexagonal phase region on the left side of the $B\mu E$ phase channel in the PE/PEO/PE–PEO system. They performed visual oil bath measurements to determine the right boundary of the $B\mu E$ phase channel. In our experiments, cloud point determinations are not so reliable for ternary mixtures close to the $B\mu E$ phase channel with relatively high block copolymer concentrations, which require longer experimental times to reach equilibrium. Therefore, it is possible that the sample, which was assigned to be purely $B\mu E$ at low temperatures according to the SANS results, could actually be macrophase separated with a hexagonal phase coexisting with one or two homopolymer-rich phases. Moreover, it should be noted that the Hex–disorder transition line in the isopleth turned upward with increasing ϕ_H . With this trend, the Hex–disorder ($B\mu E$) transition line would extrapolate to intersect with the one-phase/macrophase-separated boundary at higher ϕ_H . Thus, we hypothesize that a more correct description of the isopleth phase diagram for the PE/PEO/PE–PEO system would be that the $B\mu E$ phase channel is cut off by the hexagonal phases at low temperatures, which would be rather consistent with the current system (PEP/PBO/PEP–PBO).

When ϕ_H is decreased, the $B\mu E$ –Hex transition line extends into the ordering region of the isopleth and transforms into a Lam–Hex transition line, which provides a clue as to why the $B\mu E$ phase becomes unstable relative to the hexagonal phase as the temperature is lowered. Adding homopolymers into the diblock copolymer swells the lamellae and thereby increases the lamellae spacing. At high temperatures, for example, 120 °C, the $B\mu E$ forms when the lamellar spacing grows to approximately the curvature radius of the fluctuating lamellar interfaces, and thereby, the fluctuation effect is sufficiently strong to break up the lamellar phase.¹⁵ Whereas, at low temperatures, below 110 °C, the swelling of the lamellar phase leads to a phase transition into a hexagonal phase, prior to the theoretically predicted three-phase coexistence of the lamellar phase and two homopolymer-rich phases.^{15,32} This order–order phase transition should be essentially uncorrelated to the fluctuation effect, which generally induces the random interfaces of microstructures at certain cases, such as the sponge phase in water/surfactant system. Along the isopleth, the transition from the symmetric lamellar phase to the hexagonal phase, which is asymmetric in a geometrical sense, must be associated with the

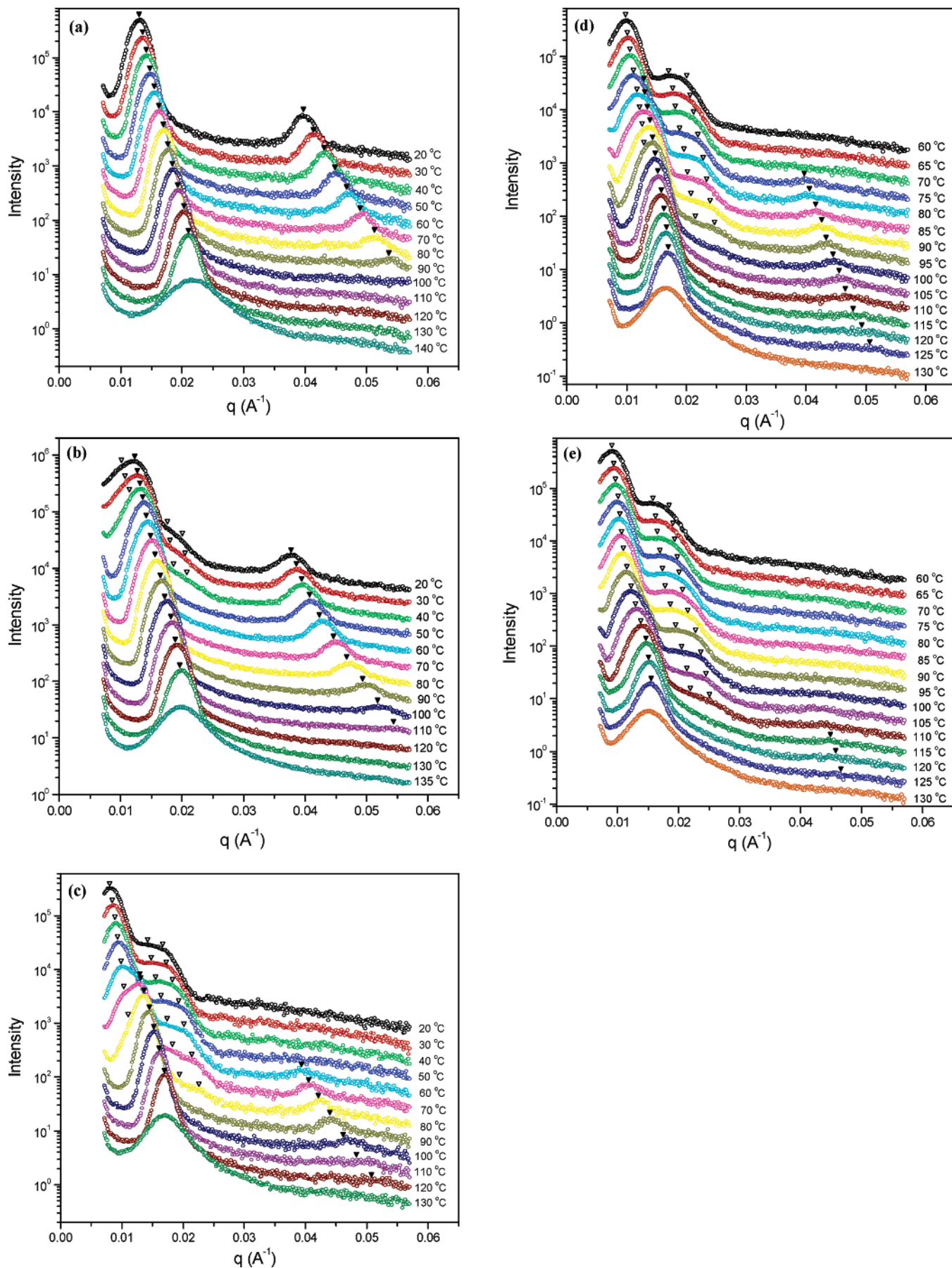


Figure 7. Cu K α SAXS data of 50/50 blends containing (a) 30%, (b) 26%, (c) 22%, (d) 20%, and (e) 18% diblock copolymers, at indicated temperatures. Curves are shifted for clarity. The filled inverted triangles represent the symmetric lamellar peaks, while the open ones indicate the hexagonal peaks.

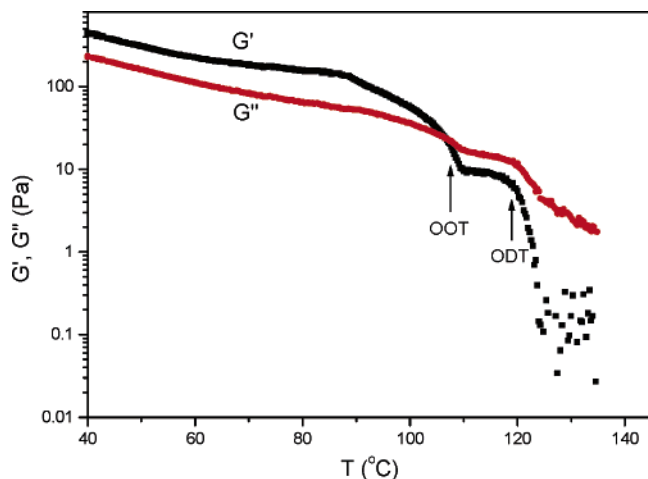


Figure 8. Dynamic temperature ramp data of the 50/50 blend containing 18% diblock copolymer. The two arrows indicate the Hex-to-Lam transition (OOT) and Lam-to-disorder transition (ODT).

dominating role of some asymmetric factor(s) in the system. We propose it is the conformational asymmetry between the PEP and PBO species that comes into play to break up the symmetry in the isopleth.

As mentioned before, conformational asymmetry has already manifested its importance in a series of phenomena. The conformational asymmetry can be quantified by a parameter¹⁷

$$\epsilon = \frac{(R_g^2/V_{\text{mol}})_A}{(R_g^2/V_{\text{mol}})_B} = \frac{\beta_A}{\beta_B} \quad (4)$$

where R_g is the radius of gyration, V_{mol} is the molecular volume of a polymer chain, and β is therefore a measure of flexibility. In previous theoretical investigations of the homopolymer A/homopolymer B/block copolymer A–B ternary blends, this effect was not taken into account.^{33–35} In our system, PBO is more flexible (lower β) than PEP, and thereby, the former appears as a shorter, “thicker” molecule while the latter looks relatively longer and “thinner”. We propose that this conformational asymmetry plays the critical role in the structural transition from the symmetric, highly swollen lamellae to the hexagonal cylinders.

For the swollen lamellar phase, the translational entropy of the homopolymers produces a repulsive interaction between the copolymer monolayers while the configurational entropy of the homopolymers causes an attraction.³⁶ The former favors the swelling of the monolayers by the homopolymers whereas the latter does not. As the homopolymers PEP and PBO are confined between the monolayers, their conformations are restricted, leading to a loss of configurational entropy. Because of different chain flexibilities, the two homopolymers experience unequal conformational perturbation, which will give rise to a new, purely entropic term to modify the free energy expression of the conformationally symmetric ternary blends. This entropic term is likely responsible for the Lam–Hex phase transition with the more flexible component PBO on the inside of the curved interface. When the microstructural symmetry is broken in this way, the stiffer homopolymer PEP gains more dimensional freedom in packing the continuous matrix of the hexagonal phase to relieve the conformational restraint, which more than compensates for the more perturbed configuration of the relatively flexible homopolymer PBO. Further quantitative analysis of this new entropic term is, however, beyond the scope of this paper.

TABLE 1: Conformational Symmetry Parameters^a

polymer pair ^b	ϵ^c
PE, PEO	1.14
PEE, PDMS	1.18
PEO, PEP	1.30
PE, PEP	1.49
PEP, PBO	1.61

^a Polymer pairs are arranged in increasing conformational asymmetry from top to bottom, assuming temperature does not change this order.

^b The former species in each pair has a larger β value than the latter.

^c The ϵ value of the PEP/PBO pair is calculated at 303 K and others at 413 K. At 303 K, $100\beta_{\text{PEP}}^2/\text{\AA}^{-1} = 7.88$ and $100\beta_{\text{PBO}}^2/\text{\AA}^{-1} = 4.89$. At 413 K, $100\beta_{\text{PE}}^2/\text{\AA}^{-1} = 9.84$, $100\beta_{\text{PEO}}^2/\text{\AA}^{-1} = 8.60$, $100\beta_{\text{PEP}}^2/\text{\AA}^{-1} = 6.61$, $100\beta_{\text{PEE}}^2/\text{\AA}^{-1} = 4.87$, and $100\beta_{\text{PDMS}}^2/\text{\AA}^{-1} = 4.11$. Molecular parameters for the calculation of β^2 are from refs 37–39.

It is straightforward to expect that the depth of $B\mu E$ phase channels might depend, at least partially, on the degree of the conformational asymmetry of systems. In Table 1, we list the ϵ values of all polymer pairs involved in our previous studies of polymeric $B\mu E$. The system PEO/PE/PEO–PE is the least conformationally asymmetric and our new system PEP/PBO/PEP–PBO is the most. Although the former is conformationally almost symmetric, there is experimental evidence⁴ to demonstrate that the $B\mu E$ phase channel is still cut off by a hexagonal phase, suggesting that a little conformational asymmetry can have dramatic effect on the phase behavior of these ternary mixtures. Among the previously investigated systems, that is, PE/PEP/PE–PEP, PEO/PEP/PEO–PEP, PEO/PE/PEO–PE, and PEE/PDMS/PEE–PDMS, we anticipate that the $B\mu E$ phase channels will eventually be cut off by hexagonal PEP-cylindrical, PEP-cylindrical, PEO-cylindrical, and PDMS-cylindrical phases, respectively.

Besides conformational asymmetry, there is one other asymmetric factor in the PEP/PBO/PEP–PBO system, which might account for the formation of the hexagonal phase in the isopleth. Along the isopleth, equal amounts of the two homopolymers would swell the respective domains of the diblock copolymer to different degrees due to the different structural natures of the two monomers, leading to a slightly asymmetric lamellar phase (The Cu $K\alpha$ SAXS results indicate that the lamellar phases in the isopleth are symmetric or nearly symmetric since the second higher-order peaks were not observed within the instrumental resolution.) To achieve a perfectly symmetric condition, this small difference in the swelling ability of the two homopolymers can be balanced by slightly adjusting the ratios of the two homopolymers. As a consequence, in the three-component phase prism, the hexagonal phase regions of two types, PBO-cylindrical and PEP-cylindrical, should be symmetric to a reflection plane, which corresponds to an absolutely symmetric lamellar phase. However, as evidenced in the Experimental Section, the same type of hexagonal phase, PBO forming the core of the cylinder, spans a wide range of the homopolymer PBO/PEP ratios from 40:60 to 60:40, suggesting that the possible asymmetric swelling ability of the two homopolymers is not responsible for the formation of the hexagonal phase.

As the homopolymer PBO/PEP ratio is varied, the left and right boundaries of the $B\mu E$ phase channel move differently. To illustrate that, the experimental part of the isothermal phase diagram at 120 °C is shown in Figure 9. The binary homopolymer blends at the PBO/PEP ratio of 45:55 require the most block copolymer to saturate the PEP/PBO interface and reduce the interfacial tension to virtually zero so as to prevent macroscopic phase separation. This suggests that the diblock copolymer is slightly more soluble in PEP than PBO and the tie lines in the

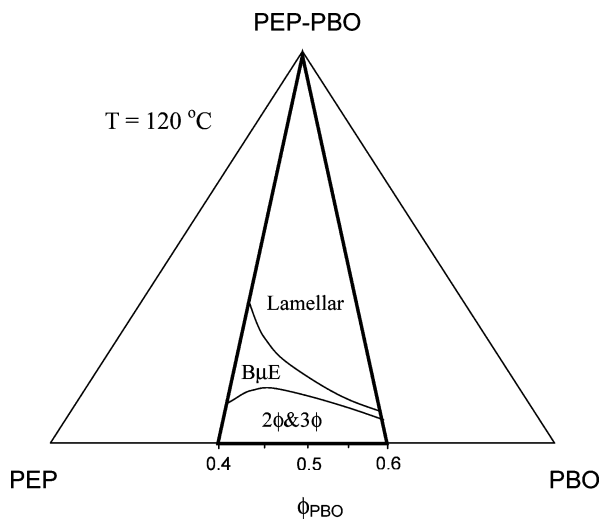


Figure 9. Isothermal phase diagram for the PEP/PBO/PEP–PBO system at 120 °C. The experimentally accessed part is marked out by a darker triangle.

macrophase-separation region of the isothermal phase diagram should decline toward the PBO corner. The PBO/PEP binodal curve shown in Figure 2 is slightly asymmetric with a critical composition $\phi_{\text{PBO}} = 0.52$, implying PBO is virtually a smaller molecule in mixing than PEP and thus the former would be a better solvent for the diblock copolymer than the latter. However, the solubility of the diblock copolymer in the homopolymers also depends on its composition. The block copolymer is a bit asymmetric in composition with $f_{\text{PBO}} = 0.49$, which accounts for its slight preferential solubility in PEP.

The left boundary of the $B\mu E$ phase channel coincides with the lamellar phase melting by swelling with the homopolymers. As illustrated in Figure 9, this boundary moves to the higher fraction of the total homopolymers as the PBO/PEP ratio is increased. The transition from a lamellar to a $B\mu E$ phase has long been investigated in the amphiphilic community. A criterion for this transition has been well established that it occurs when the interlamellar spacing reaches^{40–42}

$$\xi_{\bar{\kappa}} = a \exp\left(-\frac{6\pi}{5k_{\text{B}}T}\bar{\kappa}\right) \quad (5)$$

where a is a molecular length scale and $\bar{\kappa}$ is the membrane saddle-splay rigidity constant. This mechanism would also be applicable for the polymeric system. Recently, by using self-consistent field theory, Matsen⁴³ calculated the $\bar{\kappa}$ of a diblock copolymer monolayer in the homopolymer A/homopolymer B/diblock copolymer A–B system, that is

$$\bar{\kappa} = \rho_0 k_{\text{B}} T N^{1/2} b^3 \bar{K} \quad (6)$$

where ρ_0 , N , and b are the density, the number of the repeat units of the block copolymer, and the statistical segmental length (assuming conformational symmetry), respectively. \bar{K} is a dimensionless quantity and negative in value, only depending on χN and the ratio of the molecular weight of the homopolymer to the diblock copolymer.⁴³ Now, we are in a good position to interpret why the ternary mixtures with increasing PBO/PEP ratio need more homopolymers to break up the lamellar phase to form a fluctuation-induced microemulsion. As demonstrated in eq 6, $\bar{\kappa}$ has a strong dependence on the segmental length b , which can reflect the flexibility of a polymer chain (assuming common segment volume v_0 , $\beta^2 = b^2/6v_0 \propto b^2$). Since PBO is more flexible (lower b , and thus lower $\bar{\kappa}$) than PEP, the PBO

domain of the lamellar phase is easier to melt with the addition of the homopolymers than the PEP domain in terms of eq 5. Along the isopleth, the symmetric lamellar phase will melt only when both of the PEP and PBO layer thicknesses swell above their respective critical spacings, $\xi_{\bar{\kappa}}$. Therefore, the lamellar phase melting is determined by swelling of the mechanically harder PEP domain. Increasing the PBO/PEP ratio to the lower PEP content of the total homopolymers leads to a less effective swelling of the block copolymer toward melting into a microemulsion, and thus, more homopolymers are required for the formation of microemulsions.

Conclusions

A new polymeric system, PEP/PBO/PEP–PBO, was designed to investigate the $B\mu E$ phase channel more closely. It turns out that the $B\mu E$ phase channel in this system is eventually cut off by a hexagonal packed cylindrical phase with the more flexible component PBO constructing the core of the cylinders, which is attributed to the dramatic effect of the conformational asymmetry of the system. This feature, along with the Lam–Hex phase transition, is an important complement to the previously established universal isopleth phase diagram of the A/B/A–B system. Our findings identify another key control parameter, *conformational asymmetry*, for the practical design of polymeric $B\mu E$.

Acknowledgment. This work was supported primarily by the MRSEC Program of the National Science Foundation under Award No. DMR-0212302.

References and Notes

- Scriven, L. E. *Nature* **1976**, *263*, 123.
- Bates, F. S.; Maurer, W. W.; Lipic, P. M.; Hillmyer, M. A.; Almdal, K. S.; Mortensen, K.; Fredrickson, G. H.; Lodge, T. P. *Phys. Rev. Lett.* **1997**, *79* (5), 849.
- Fredrickson, G. H.; Bates, F. S. *J. Polym. Sci., Part B: Polym. Phys.* **1997**, *35*, 2775.
- Hillmyer, M. A.; Maurer, W. W.; Lodge, T. P.; Bates, F. S.; Almdal, K. *J. Phys. Chem. B* **1999**, *103* (23), 4814.
- Washburn, N. R.; Lodge, T. P.; Bates, F. S. *J. Phys. Chem. B* **2000**, *104* (30), 6987.
- Schwahn, D.; Mortensen, K.; Frielinghaus, H.; Almdal, K.; Kielhorn, L. *J. Chem. Phys.* **2000**, *112*, 5454.
- Lee, J. H.; Balsara, N. P.; Krishnamoorthi, R.; Jeon, H. S.; Hammouda, B. *Macromolecules* **2001**, *34*, 6557.
- Corvazier, L.; Messe, L.; Salou, C. L. O.; Young, R. N.; Fairclough, J.; Ryan, A. J. *J. Mater. Chem.* **2001**, *11*, 2864.
- Krishnan, K.; Almdal, K.; Burghardt, W. R.; Lodge, T. P.; Bates, F. S. *Phys. Rev. Lett.* **2001**, *87* (9), 098301.
- Kodama, H.; Komura, S.; Tamura, K. *Europhys. Lett.* **2001**, *53* (1), 46.
- Caputo, F. E.; Burghardt, W. R.; Krishnan, K.; Bates, F. S.; Lodge, T. P. *Phys. Rev. E* **2002**, *66*, 041401.
- Burghardt, W. R.; Krishnan, K.; Bates, F. S.; Lodge, T. P. *Macromolecules* **2002**, *35* (10), 4210.
- Messe, L.; Corvazier, L.; Ryan, A. J. *Polymer* **2003**, *44*, 7393.
- Lee, J.; Rugg, M. L.; Balsara, N. P.; Zhu, Y.; Gido, S. P.; Krishnamoorthi, R.; Kim, M. H. *Macromolecules* **2003**, *36*, 6537.
- Duchs, D.; Ganesan, V.; Fredrickson, G. H.; Schmid, F. *Macromolecules* **2003**, *36*, 9237.
- Duchs, D.; Schmid, F. *J. Chem. Phys.* **2004**, *121* (6), 2798.
- Fredrickson, G. H.; Donley, J. P. *J. Chem. Phys.* **1992**, *97* (12), 8941.
- Wu, D.; Fredrickson, G. H. *J. Chem. Phys.* **1996**, *104* (16), 6387.
- Sikka, M.; Singh, N.; Karim, A.; Bates, F. S.; Satija, S. K.; Majkrzak, C. F. *Phys. Rev. Lett.* **1993**, *70* (3), 307.
- Bates, F. S.; Fredrickson, G. H. *Macromolecules* **1994**, *27*, 1065.
- Vavasour, J. D.; Whitmore, M. D. *Macromolecules* **1993**, *26*, 7070.
- Matsen, M. W.; Schick, M. *Macromolecules* **1994**, *27*, 4014.
- Matsen, M. W.; Bates, F. S. *J. Polym. Sci., Part B: Polym. Phys.* **1997**, *35*, 945.
- Singh, C.; Schweizer, K. S. *Macromolecules* **1997**, *30*, 1490.
- Zhou, N.; Bates, F. S.; Lodge, T. P. Manuscript in preparation.

- (26) Wignall, G. D.; Bates, F. S. *J. Appl. Crystallogr.* **1987**, *20*, 28.
- (27) Flory, P. J. *Principles of Polymer Chemistry*; Cornell University Press: New York, 1953.
- (28) Stanley, H. E. *Introduction to Phase Transitions and Critical Phenomena*; Oxford University Press: New York, 1971.
- (29) After the blends were prepared, they stayed at room temperature for days before the cloud point determination. So, if their cloud points were above RT, then the blends were cloudy enough so that the phase separation could be observed under an optical microscope.
- (30) Teubner, M.; Strey, R. *J. Chem. Phys.* **1987**, *87*, 3195.
- (31) Schubert, K.-V.; Strey, R.; Kline, S. R.; Kaler, E. W. *J. Chem. Phys.* **1994**, *101*, 5343.
- (32) Naughton, J. R.; Matsen, M. W. *Macromolecules* **2002**, *35*, 8926.
- (33) Janert, P. K.; Schick, M. *Macromolecules* **1997**, *30*, 137.
- (34) Kielhorn, L.; Muthukumar, M. *J. Chem. Phys.* **1997**, *107* (14), 5588.
- (35) Huh, J.; Jo, W. H. *J. Chem. Phys.* **2002**, *117* (21), 9920.
- (36) Thompson, R. B.; Matsen, M. W. *J. Chem. Phys.* **2000**, *112* (15), 6863.
- (37) Matsushima, M.; Fukatsu, M.; Kurata, M. *Bull. Chem. Soc. Jpn.* **1968**, *41*, 2570.
- (38) Fetters, L. J.; Lohse, D. J.; Richter, D.; Witten, T. A.; Zirkel, A. *Macromolecules* **1994**, *27* (17), 4639.
- (39) Almdal, K.; Hillmyer, M. A.; Bates, F. S. *Macromolecules* **2002**, *35*, 7685.
- (40) Golubovic, L. *Phys. Rev. E* **1994**, *50*, R2419.
- (41) Morse, D. C. *Phys. Rev. E* **1994**, *50*, R2423.
- (42) Gompper, G.; Kroll, D. M. *Phys. Rev. Lett.* **1998**, *81*, 2284.
- (43) Matsen, M. W. *J. Chem. Phys.* **1999**, *110* (9), 4658.